Growth rate and morphology of isotactic polystyrene crystals in solution at high supercoolings

Yasutoshi Tanzawa*
Department of Physics, Faculty of Science, Kyoto University, Kyoto 606, Japan
(Received 13 May 1991; revised 19 July 1991; accepted 8 August 1991)

The morphology and temperature dependence of the lateral growth rate G are reported for isotactic polystyrene crystallized from 0.1% dimethyl phthalate solution at high supercoolings. The outline of a lamella is a rounded hexagon for the highest temperature and a ragged circle for lower temperatures. The edges of the lamellae become ragged and overgrowth is pronounced with decreasing temperature. A linear relationship is found between $\log(G/\eta)$ and $1/T\Delta T$ over a wide range of supercooling ($\Delta T = T_d^\circ - T$) from 70 to 170 K, where η is a retardation factor of Arrhenius form with an activation energy of 8400 K, and T_d° is the equilibrium dissolution temperature. The value of T_d° is determined to be 200°C by differential scanning calorimetry. In these high supercoolings, the nucleation theory of polymer crystallization loses its validity; in fact, the slope of the plot of $\log(G/\eta)$ *versus* $1/T\Delta T$ is four times as large as the value predicted by nucleation theory. Possible growth mechanisms at high supercoolings are discussed on the basis of the morphology.

(Keywords: growth rate; morphology; high supercooling; isotactic polystyrene; dimethyl phthalate)

INTRODUCTION

The growth rate G of polymer crystals has been well described by the following equation[1]:

$$\log G = \log G_0 + \log \eta - \frac{K_j}{T\Delta T} \tag{1}$$

where G_0 and K_j are constants, η is a retardation or viscosity factor and can be expressed by an Arrhenius or WLF-type function, and ΔT ($=T_d^\circ - T$) is a supercooling (T_d° is the equilibrium dissolution temperature). For melt crystallization, T_d° should be replaced by the equilibrium melting temperature T_m°. The subscript j in K_j represents the growth regime, i.e. j = I, II or III.

According to nucleation theory[2], the two-dimensional nucleation rate i is given by the following equation:

$$\log i \sim -\frac{4b\sigma\sigma_e T_d^\circ}{k\Delta h_f T\Delta T} \tag{2}$$

where b is the thickness of a nucleus, and σ and σ_e are the side- and end-surface free energy per unit area, respectively, Δh_f is the heat of dissolution per unit volume of crystal and k is the Boltzmann constant. Seto[3] and Frank[4] showed that, in regime II, $G \sim (ig)^{1/2}$ where g is the propagation velocity of steps. Since g is assumed to be independent of temperature, K_{II} is represented by the following equation:

$$K_{II} = \frac{2b\sigma\sigma_e T_d^\circ}{k\Delta h_f} \tag{3}$$

where $K_I = 2K_{II}$ (ref. 4) and, according to Hoffman[5], $K_{III} = 2K_{II}$.

However, it should be noted that there is a lower limit of crystallization temperature below which nucleation theory cannot be applied.

We estimate a limiting temperature T^* at which the width of a critical nucleus becomes that of one stem; T^* is the lowest temperature at which nucleation theory may hold. Following nucleation theory[2], the number of stems in a critical nucleus v^* decreases with ΔT as follows:

$$v^* = \frac{2\sigma T_d^\circ}{a\Delta h_f \Delta T} \tag{4}$$

where a is the width of a stem. Here, we neglect the temperature dependence of Δh_f and the entropy of fusion for simplicity. Substituting 1 for v^* in equation (4), we obtain the limiting supercooling ΔT^* ($=T_d^\circ - T^*$) from the following equation:

$$\frac{\Delta T^*}{T_d^\circ} = \frac{2\sigma}{a\Delta h_f} \tag{5}$$

For isotactic polystyrene (iPS), we estimate the value of the right-hand side of equation (5) to be 0.15 by using the parameters in *Table 1*; T^* = 120°C for crystallization from a 0.1% dimethyl phthalate (DMP) solution and T^* = 160°C for crystallization from the melt. For polyethylene (PE), the value of $2\sigma/a\Delta h_f$ is 0.22; T^* = 28°C for crystallization from a dilute xylene solution and T^* = 54°C for crystallization from the melt. Therefore, iPS can be crystallized isothermally below T^*; the growth rate of PE is too fast to crystallize isothermally at such high supercooling.

*Present address: Department of Systems Engineering, Nagoya Institute of Technology, Gokiso, Showa-ku, Nagoya 466, Japan

0032-3861/92/132659-07

Table 1 Values of the parameters for crystallization from the melt

$\sigma\sigma_e$ ($\times 10^{-14}$ J^2 cm^{-4})	Δh_f (J cm^{-3})	σ_e ($\times 10^{-7}$ J cm^{-2})	T_m° (°C)	a (Å)	b (Å)
133	91.1[a]	28.8[b]	242[a]	6.4	11.0

[a]From ref. 9
[b]From ref. 13

Lamellar thickness at high supercoolings has been studied[6–8] to confirm the deviation from nucleation theory; the lamellar thickness is represented by an exponential function of $1/T$ at high supercoolings. The crystallization rate was also measured by laser transmittance through the crystal suspension[6,7]. However, since the relationship between transmittance and lamellar size was not known, the growth rate was not obtained.

In this paper, the growth rate for crystallization from a 0.1% DMP solution is determined by observing the lateral size of lamellae by transmission electron microscopy (TEM) to confirm the deviation from nucleation theory at high supercoolings beyond ΔT^*. On the basis of the morphology of the iPS crystals, alternative mechanisms are discussed.

EXPERIMENTAL

Materials

The iPS and DMP used were commercially obtained and are the same as those in preceding papers[7,8]. The original iPS had an average molecular weight of 1.57×10^6 ($M_w/M_n = 6.4$) with a tacticity of 97.2% triads.

Determination of the equilibrium dissolution temperature

We determined the equilibrium dissolution temperature of iPS in DMP solution using a differential scanning calorimeter (Rigaku 10A). Samples were prepared as follows. First, crystallization was carried out from 10% DMP solution at 130°C. After crystallization, the resulting suspension was gel-like. Then the solvent DMP in the gel-like sample was substituted by methyl ethyl ketone (MEK). The sample dried in air was annealed in Ar atmosphere at several temperatures up to 220°C. The iPS sample was placed in an aluminium pan for d.s.c. measurements with a certain amount of DMP so that the concentration of the solution was $10 \pm 1\%$ or $2 \pm 0.5\%$ after dissolution. The pan was hermetically sealed in air.

Crystallization and electron microscopy

Crystallization was carried out in the 0.1% DMP solution. First, iPS was dissolved in DMP at 200°C for 1 h with gentle stirring under N_2 atmosphere. The solution was quenched to a crystallization temperature T_c from 30 to 130°C. This procedure decreases the molecular weight of crystallized iPS to 4.4×10^5 ($M_w/M_n = 3.7$)[7]. During crystallization, a sheet of carbon-coated mica fixed to a Teflon stick was dipped in the solution for sampling iPS crystals. After a suitable period, this mica sheet was removed from the solution and a new sheet was dipped. These procedures were repeated several times. Then the mica sheet was dipped in MEK at room temperature to remove residual DMP and uncrystallized iPS, dried in air, and shadowed by Pt–Pd. The iPS crystals on the carbon film were observed by TEM. The growth rate was determined from the initial slope of the time–radius curve.

RESULTS

Dissolution temperature

Figure 1 shows typical d.s.c. thermograms of unannealed samples on melting and dissolution. *Figure 1a* shows typical double melting peaks. The higher melting peak (~220°C) corresponds to the melting of lamellae thickened during the heating process and the lower one corresponds to the melting of unthickened lamellae. The lower peak temperature was taken as the melting temperature T_m of as-crystallized lamellae and the lamellar thickness was calculated using the parameters in *Table 1* and the following equation:

$$l = \frac{2\sigma_e T_m^\circ}{\Delta h_f (T_m^\circ - T_m)} \tag{6}$$

On dissolution, a single peak is observed at heating rates of 20 and 1°C min^{-1} (*Figures 1b* and *c*). The peak temperatures are almost the same; the heating rate does not affect the dissolution temperature appreciably. Therefore, thickening does not occur at the slower heating rate of 1°C min^{-1}. The peak temperature in *Figure 1c* can be taken to be the dissolution temperature T_d of lamellae the thickness of which is given by equation

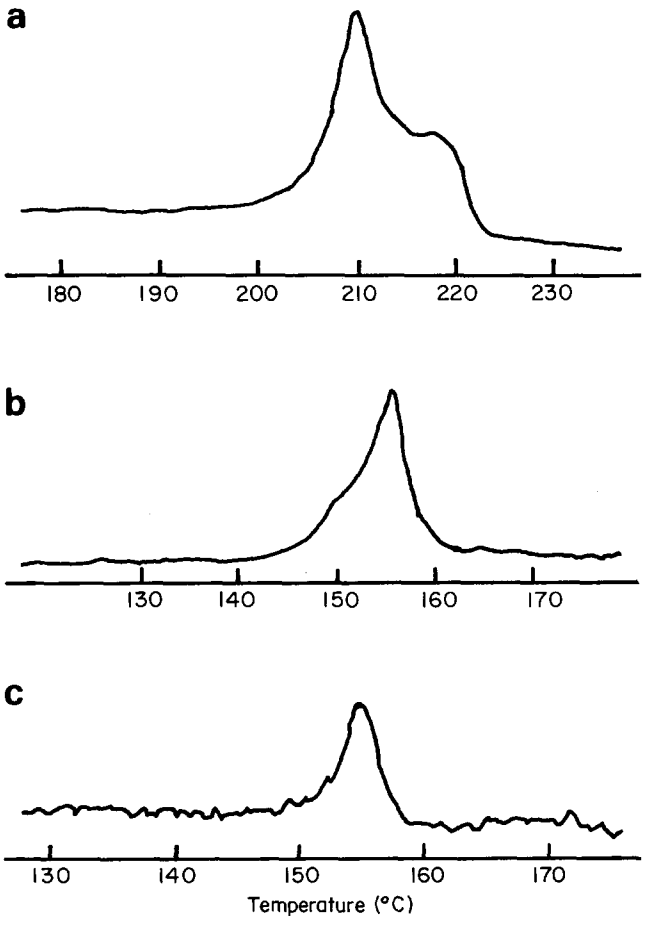

Figure 1 D.s.c. thermograms of unannealed iPS: (a) melting thermogram of unannealed sample. Heating rate 20°C min^{-1}; (b) dissolution thermogram of original suspension (iPS 10% in DMP). Heating rate 20°C min^{-1}; (c) dissolution thermogram of unannealed sample in 10% DMP solution. Heating rate 1°C min^{-1}

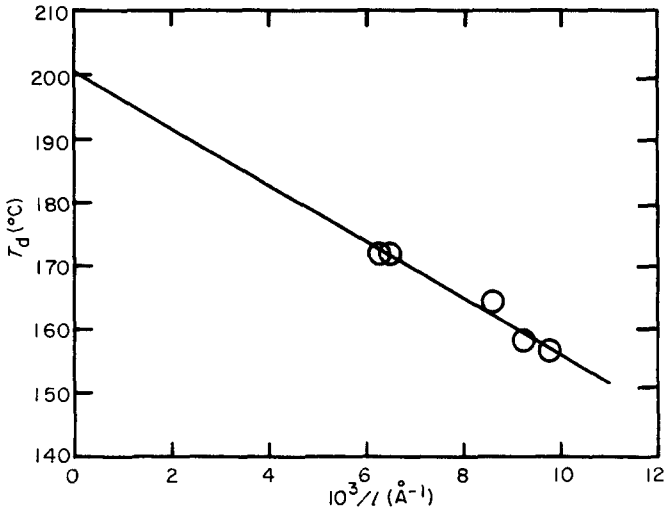

Figure 2 Dependence of T_d of iPS on inverse of lamellar thickness $1/l$ in 2% DMP solution

(6). The relationship between T_d and l is given by:

$$T_d = T_d^\circ\left(1 - \frac{2\sigma_e'}{\Delta h_f' l}\right) \tag{7}$$

where σ_e' and $\Delta h_f'$ are the values for dissolution. Using equation (7), we can determine the correct value of T_d° as far as $\sigma_e/\Delta h_f$ and $\sigma_e'/\Delta h_f'$ are constants. *Figure 2* shows the T_d *versus* $1/l$ curve for 2% solution; the curve for the 10% solution is almost the same. Extrapolating $1/l$ to zero, we determine the equilibrium dissolution temperature: 202°C and 201°C for the 10% and 2% solutions, respectively. The concentration dependence is small in this concentration range. Therefore, we adopt the value of 200°C for the dissolution temperature in a 0.1% solution. The error in this value does not affect the following discussion.

With crystallinity of ~40% calculated from the area of the melting peak, we also obtain the heat of dissolution in DMP (90–130 J cm^{-3}) from the area of the dissolution peak. The value for the heat of dissolution is 1.0–1.5 that of the heat of fusion.

Morphology

Figure 3a shows the morphology of a sample crystallized at 130°C, the highest temperature examined. Only at this temperature is the outline of the lamellae rounded hexagonal: the average ratio of the edge-to-edge distance to the apex-to-apex distance is not the value of a regular hexagon, $\cos 30^\circ = \sqrt{3}/2$, but almost 1. We confirmed by electron diffraction that the edges, which are growth surfaces, are (110) planes. These facts suggest that, at 130°C, crystals grow basically by the propagation of steps along the (110) plane.

Figure 3b shows the morphology at 100°C. This micrograph shows typical morphological features of a lamella grown at higher temperatures: (1) the crystals have rounded outlines on average; (2) the edge of each lamella is ragged; (3) there exist small apexes the angle of which is nearly 120°; (4) there are wide terraces due to less overgrowths.

With increasing temperature, the morphology changes gradually: features (1) and (2) become more conspicuous, and (3) can be hardly seen (*Figures 3c* and *d*). In particular, the edges of the lamellae are remarkably ragged at lower temperatures (*Figure 3d*). Although the ragged scale in *Figure 3d* is much larger than the molecular scale, these ragged edges suggest that the growth face is rough. In *Figure 3d*, the increasing overgrowths make the crystal look like a cluster of crystallites instead of lamellae. However, the electron diffraction (*Figure 3e*) shows that the molecular conformation of the iPS crystals is the 3_1-helix and that there exists a main lamella and the direction of overgrown crystals correlates with that of the main lamella.

The change in morphology suggests that the growth mechanism changes gradually with decreasing temperature; the growth face becomes rough on the molecular scale at lower temperatures.

Growth rate

The radius of the lamellae increases linearly with crystallization time for all crystallization temperatures as shown in *Figure 4*. The growth rate is determined from the slope of the time–radius curve (*Figure 5*). The growth rate has a maximum around 80°C. The maximum in the melt crystallization appears at ~180°C. The maximum appears due to the balance of two factors, an increasing factor including ΔT and a decreasing retardation factor with decreasing temperature. In solution, the former dominates over the latter down to a lower temperature than in the melt.

RETARDATION FACTOR

The retardation factor η has been represented by either

$$\eta = \exp\left(-\frac{E}{RT}\right) \tag{8}$$

or

$$\eta = \exp\left[-\frac{U}{R(T - T_\infty)}\right] \tag{9}$$

where E is an activation energy, U and T_∞ are constants, and R is the gas constant: equation (8) is the Arrhenius equation and equation (9) is the WLF-type equation. The experiment on dynamic viscosity suggests that the WLF equation ($U/R = 2070$ K) holds in a temperature range between the glass transition temperature T_g and $T_g + 100$ K. On the other hand, the Arrhenius equation holds for temperatures higher than $T_g + 100$ K. In almost all crystallization from the melt, the WLF-type equation has been used. However, in the case of growth from a solution, T_g would be low enough for the Arrhenius equation to be applied except in solutions with high concentrations. Therefore, we adopt the Arrhenius equation for the retardation factor.

Figure 6 shows $\log(G/\eta)$ ($=\log G + E/2.303RT$) as a function of $1/T\Delta T$ for several values of E/R. The solid lines are fitted to the data at temperatures higher than 80°C by the least square method. The values of E/R between 4500 K and 8400 K are examined; $E/R = 8400$ K gives the best fitting to give a linear function for the whole temperature range studied. The values smaller than 4500 K are unreasonable because $\log(G/\eta)$ decreases with decreasing temperature in the lowest temperature region. For the values larger than 8400 K, this plot rises in the lower temperature region. This upswing is not the

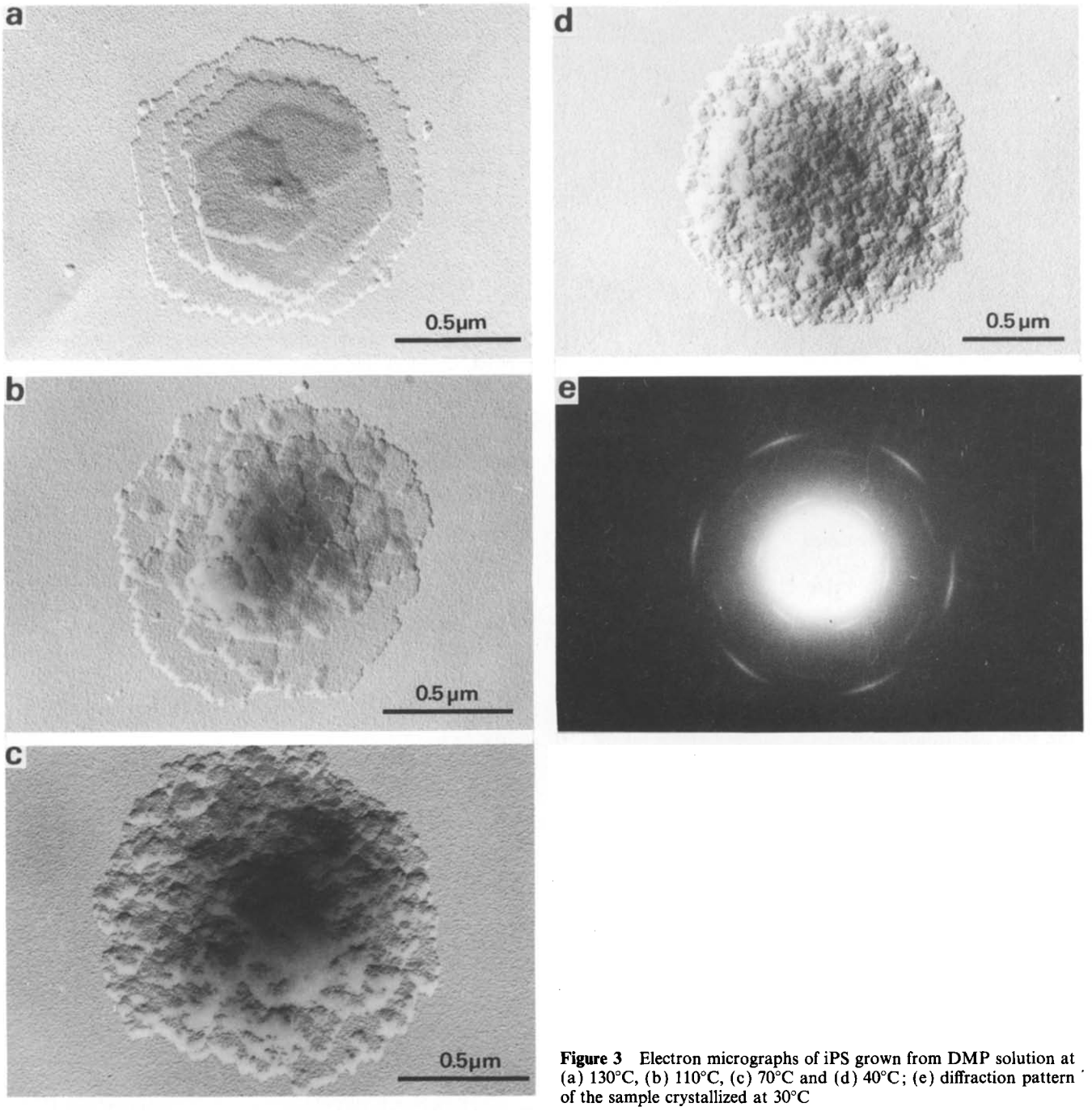

Figure 3 Electron micrographs of iPS grown from DMP solution at (a) 130°C, (b) 110°C, (c) 70°C and (d) 40°C; (e) diffraction pattern of the sample crystallized at 30°C

regime transition but the overestimation of the value of E/R. Therefore, the value of E/R should be between 4500 K and 8400 K. Since the fitting by a linear function is very good and, at present, we have no evidence for the change in growth mechanism within the temperature range examined, we mainly adopt the value of 8400 K for the activation energy E/R in the following discussion. This selection means that $\log(G/\eta)$ depends on $1/T\Delta T$ linearly over the whole temperature range examined; equation (1) holds from 30 to 130°C. It is to be noted that, as shown in *Figure 6*, the slopes of the fitted lines are almost the same within 25% for the different values of E/R. Therefore, the following discussion holds its validity irrespective of the value of E/R, if we restrict the temperature range above 80°C.

ANALYSIS BASED ON NUCLEATION THEORY

Since the growth of iPS from a 0.1% DMP solution is extremely slow at high temperatures where nucleation is sure to be the rate-determining process, the thermodynamic parameters, such as σ and σ_e, have not been determined experimentally. Therefore, we assume that, except for T_d°, the parameters are the same as those for melt growth. In fact, this assumption holds in the case of PE. In *Table 1*, the values of the parameters are listed. Here, we comment on the value of $\sigma\sigma_e$. As pointed out by Hoffman[1], the value obtained by Suzuki and Kovacs[9] should be doubled on the basis of regime II growth: $\sigma\sigma_e$ is 266×10^{-14} J^2 cm^{-4}. However, the folding trajectory also should be taken into consideration; {330} folding[11] gives $b = 5.5$ Å and zigzag folding[12] gives 11.0 Å. In the

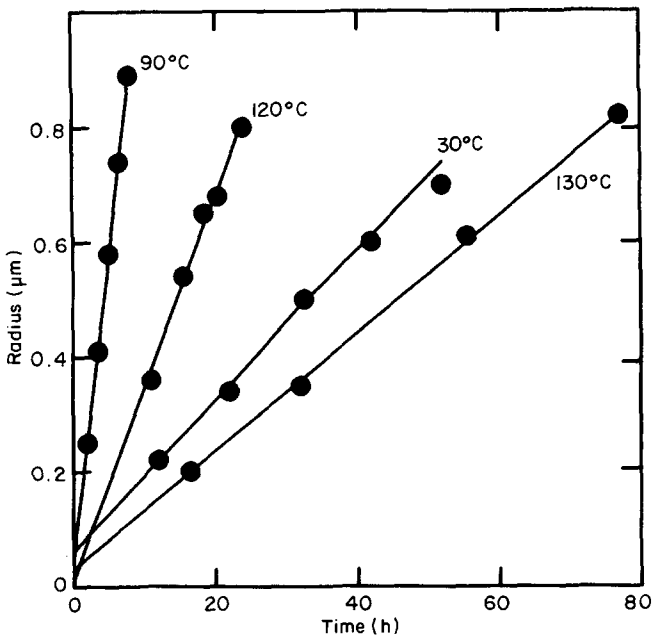

Figure 4 Time dependence of lateral size of lamella for several crystallization temperatures

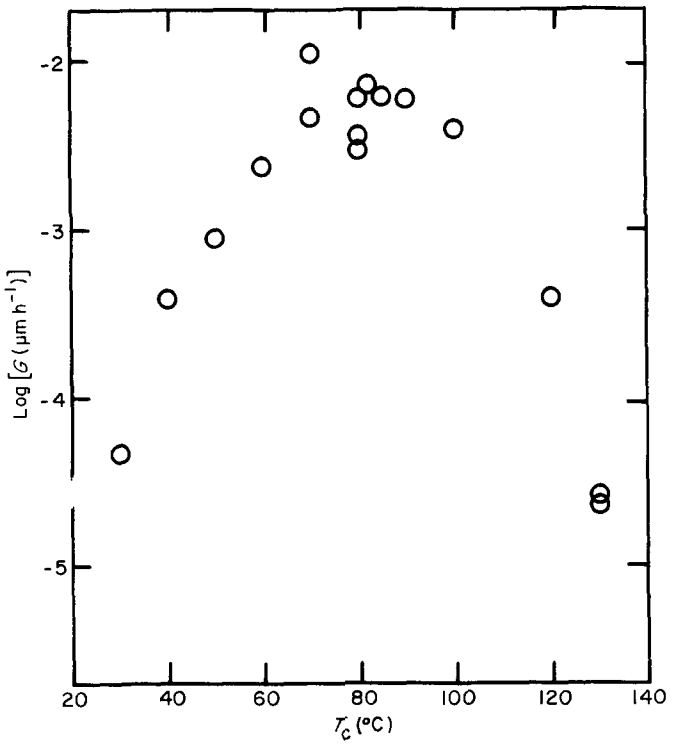

Figure 5 Dependence of growth rate on crystallization temperature T_c

case of {330} folding, the first layer has only one nearest neighbour chain as shown in *Figure 7a*. Therefore, it is reasonable to assume that growth strip spreads out by zigzag folding (*Figure 7b*). Accordingly, we get $\sigma\sigma_e = 133 \times 10^{-14}$ J^2 cm^{-4} again with $b = 11.0$ Å from equation (3). (The values for a and b are listed in *Table 1*.)

Using the parameters in *Table 1*, we compare the results from this work and those of melt growth[9,13] in the light of the growth in regime II, since the existence of regime III has not been reported for crystallization of iPS. First, we discuss the value of $\sigma\sigma_e/\Delta h_f$. Since $\log(G/\eta)$ depends on $1/T\Delta T$ linearly, we can calculate the value of $\sigma\sigma_e/\Delta h_f$ from the slope of the $\log(G/\eta)$ *versus* $1/T\Delta T$ curve if we assume that equation (3) holds. The value obtained in this work is four times as large as that of melt growth as shown in *Table 2*. (Even if we assume regime III, it is still two times larger.) If the entropy term of σ is neglected, σ is proportional to Δh_f. Therefore, $\sigma/\Delta h_f$ remains constant; the value of σ_e in this work must be four times as large as that of melt growth for regime II.

Now we discuss the dependence of lamellar thickness on supercooling and compare the value of $\sigma_e/\Delta h_f$ with that in the melt growth. It has been shown[6–8] that, at high supercoolings, lamellar thickness depends on crystallization temperature as follows

$$l = \delta l + A_1 \exp\left(-\frac{B_1}{T}\right) \qquad (10)$$

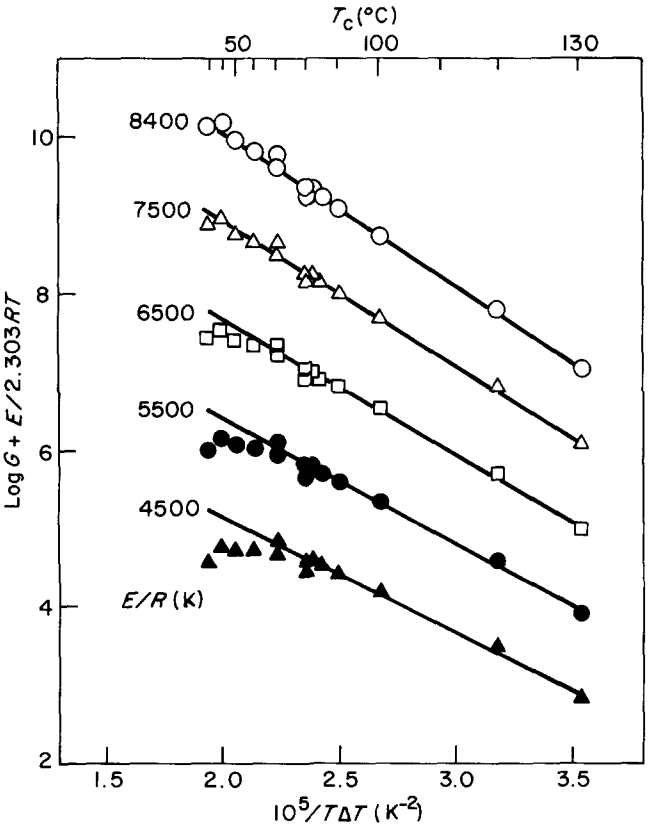

Figure 6 Dependence of $\log(G/\eta)$ on $1/T\Delta T$ for several values of E/R. Solid line is fitted above 80°C

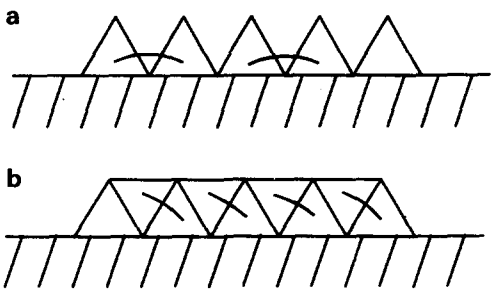

Figure 7 Schematic figure of growth surface of iPS at low supercooling: (a) {330} folding; (b) zigzag folding

Table 2 Thermodynamic parameters of iPS from nucleation theory

	This work (A)	Melt growth (B)	Ratio (A/B)
$\sigma\sigma_e/\Delta h_f$ (J cm^{-1})	6.01	1.46[a]	4.1
$\sigma_e/\Delta h_f$ (Å)	1.29	3.16[b]	0.41
σ ($\times 10^{-7}$ J cm^{-2})	46.6	4.62	10.1

[a]From ref. 9
[b]From ref. 13

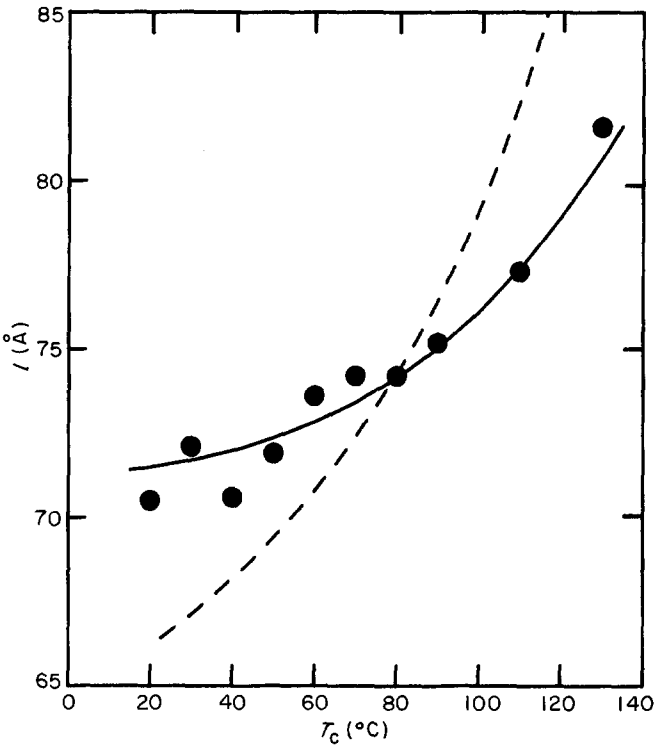

Figure 8 Dependence of lamellar thickness l on crystallization temperature T_c: (○) experimental data from reference 7; (——) equation (10) with δl = 71 Å, A_1 = 27 000 Å and B_1 = 3200 K; (– – –) equation (11) with the parameters in *Table 1* and δl = 50 Å

where δl, A_1 and B_1 are constants (see refs 6 and 7 for the detailed form of δl, A_1 and B_1). On the other hand, nucleation theory gives the following equation:

$$l = \delta l + \frac{2\sigma_e T_d^o}{\Delta h_f \Delta T} \qquad (11)$$

The experimental data from reference 7, equations (10) and (11) are shown in *Figure 8*. It is clearly seen that the experimental results cannot be explained by the value of $\sigma_e/\Delta h_f$ in the melt growth. However, we can fit the experimental data by equation (11), if we adopt an extremely small value of 1.29 Å for $\sigma_e/\Delta h_f$; this value is 0.4 of the usual value (*Table 2*).

Table 2 also lists the values of σ calculated from the above two quantities, $\sigma\sigma_e/\Delta h_f$ and $\sigma_e/\Delta h_f$. The ratio of σ in the present work to that of the melt crystallization is 10; we cannot accept this result. If the value of σ was 10 times larger, the value of Δh_f would be 10 times larger too as discussed above; this effect must be observed by the d.s.c. experiment. However, the value obtained for Δh_f for dissolution in DMP was 90–130 J cm^{-3}. This value is only 1.0–1.5 times larger than that for melting. In conclusion, we cannot explain the dependence of both the growth rate and lamellar thickness at high supercoolings in terms of the present nucleation theory.

DISCUSSION

The growth mechanism at high supercoolings on the basis of the linear relation between $\log(G/\eta)$ and $1/T\Delta T$ has been discussed. In this paper, the Arrhenius equation, equation (7), is used for the retardation factor η, and an activation energy of 8400 K gives a linear relationship over the whole temperature range examined. Since the plot of $\log(G/\eta)$ against $1/T\Delta T$ is represented by a straight line, it is natural to expect that the growth mechanism does not change in the supercooling range studied. However, we must emphasize that the temperature range in which nucleation theory is valid has a lower bound T^*. Although this situation has not been pointed out, the existence of a lower bound T^* is very important to confirm the validity of nucleation theory. Therefore, we have to construct a new theory which has no bounds in the temperature range and gives the same dependence on temperature at both low and high supercoolings. In this case, equation (3) loses its validity; we have to use a new expression for the parameter K_j in equation (1). Therefore, crystallization from the melt at high supercoolings should be re-examined in the light of the value of T^*.

Next, we discuss the approach based on adhesive growth; in adhesive growth, the rate-determining process is no longer nucleation but a folding process. It has been shown that the folding probability P_{fold} at high supercooling is represented by the following equation,

$$P_{fold} = P_0[1 - A\exp(-\beta\Delta T)] \qquad (12)$$

where P_0, A and β are constants[6]. Equation (12) is almost independent of temperature at high supercoolings; the temperature dependence of $\log(G/\eta)$ cannot be explained by equation (12). In the case of low molecular weight substances, however, it is known that the growth rate is represented by an equation similar to equation (12) at high supercoolings. In the case of a polymer, it has to be taken into consideration that crystals have to grow mainly by cilia folding; growth rate depends on not only P_{fold} but also the density of cilia which can fold, N_{cilia}, i.e. $G/\eta \propto N_{cilia}P_{fold}$. Therefore, the logarithm of N_{cilia} should depend linearly on $1/T\Delta T$ on the basis of the assumption that E/R = 8400 K. However, if we regard that $\log(G/\eta)$ is almost independent of supercooling below 80°C with E/R = 4500 K, equation (12) gives rise to constant N_{cilia}. In this case, we need both a reason why N_{cilia} changes at 80°C and an explanation for the dependence on temperature above 80°C.

There should exist a growth intermediate between nucleation-controlled growth and adhesive growth. In this case, there is no (or little) nucleation barrier for the deposition of a molecule in solution and steps are still preferred sites in the folding process. Therefore, there may exist multi-height steps and growth in another direction may occur (*Figure 9*). The origins to build a multi-height step are: (1) exhaustion of a molecule (immobile step[14]); and (2) folding to an upper growth face before the step is annihilated by running into another step. At low supercoolings, (1) only makes the propagation velocity decrease and (2) does not occur, since the nucleation rate is sufficiently small. Growth in another direction divides growth surface into small parts;

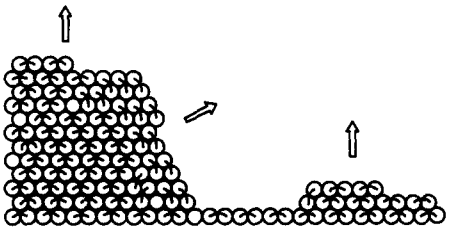

Figure 9 Schematic illustration of the growth surface. Arrows represent the direction of growth

the outline of a lamella loses its anisotropy and the edge of a lamella becomes ragged. Thus, the roughness of a lamella changes continuously with supercooling; we can explain the morphological change in *Figure 3* with this model.

At present, we have not succeeded in obtaining a unified theory which gives the linear relation between $\log(G/\eta)$ and $1/T\Delta T$, the temperature dependence of lamellar thickness, and the change in morphology in the wide range of temperature studied. There are only a few experiments on crystallization at high supercoolings. It should be emphasized, however, that the study of crystallization at high supercoolings is very important to confirm the validity of nucleation theory, as mentioned above. Therefore, crystallization at high supercoolings should be studied to recognize the growth mechanism not only at high supercoolings but also at low supercoolings.

CONCLUSIONS

We determined the equilibrium dissolution temperature of iPS in DMP solution by d.s.c.: 202°C for 10% and 201°C for 2%. The heat of dissolution in DMP solution was found to be between 1.0 and 1.5 times the heat of melting. The morphology of iPS crystals changes remarkably with crystallization temperature from 130 down to 30°C, i.e. the lamellar edge becomes ragged and overgrowth becomes pronounced with decreasing temperature. The outline of a lamella is a rounded hexagon for $T_c = 130$°C and a ragged circle for lower crystallization temperatures. The logarithm of G/η depends on $1/T\Delta T$ linearly even at very high supercoolings by using equation (7) for η; the activation energy of 8400 K gives the linear relationship over the whole temperature range studied. However, the slope obtained is so large that we cannot explain the temperature dependence of both the growth rate and lamellar thickness at high supercooling in terms of nucleation theory; σ_e would be 4 times, and σ and Δh_f would be 10 times as large as the values for the melt growth, respectively.

ACKNOWLEDGEMENTS

Special thanks go to Dr A. Toda of Kyoto University for his suggestion for the sample preparation for electron microscopy. The author also thanks Professor H. Kiho of Nagoya Gakuin University, and Professor Y. Miyamoto and H. Miyaji of Kyoto University for their valuable discussions and continuous encouragement.

REFERENCES

1 Hoffman, J. D., Davis, G. T. and Lauritzen Jr, J. I. in 'Treatise on Solid State Chemistry' (Ed. N. B. Hannary) Vol. 3, Plenum, New York, 1976, Ch. 7
2 Mandelkern, L. 'Crystallization in Polymers', McGraw-Hill, New York, 1964
3 Seto, T. *Rep. Prog. Polym. Phys. Jpn* 1964, **7**, 67
4 Frank, F. C. *J. Cryst. Growth* 1974, **22**, 233
5 Hoffman, J. D. *Polymer* 1983, **24**, 3
6 Kiho, H., Miyamoto, Y. and Miyaji, H. *Polymer* 1986, **27**, 1505
7 Tanzawa, Y., Miyaji, H., Miyamoto, Y. and Kiho, H. *Polymer* 1988, **29**, 904
8 Miyamoto, Y., Tanzawa, Y., Miyaji, H. and Kiho, H. *J. Phys. Soc. Jpn* 1989, **58**, 1879
9 Suzuki, T. and Kovacs, A. J. *Polym. J.* 1970, **1**, 82
10 Adam, G. and Gibbs, J. H. *J. Chem. Phys.* 1965, **43**, 139
11 Guenet, J. M. *Macromolecules* 1980, **13**, 389
12 Sadler, D. M., Spells, S. J., Keller, A. and Guenet, J. M. *Polym. Commun.* 1984, **25**, 290
13 Edwards, B. C. and Phillips, P. J. *Polymer* 1974, **15**, 351
14 Toda, A., Kiho, H., Miyaji, H. and Asai, K. *J. Phys. Soc. Jpn* 1985, **54**, 1411